CHALMERS
UNIVERSITY OF TECHNOLOGY

Test Zone Verification Procedures in a Random-LOS Measurement Setup

Correction for the paper "Test Zone Verification Procedures in a Random-LOS Measurement Setup", EuCAP 2019

Corrections compared to the published paper in the EuCAP 2019 proceedings and on IEEE.

- Figures 3-4: The y-axis in the figures were a factor 2 wrong.
- The definition of P in Section III is revised, a sum has been removed.

Here follows the corrected paper with the correct figures.

Test Zone Verification Procedures in a Random-LOS Measurement Setup

Madeleine Schilliger Kildal[1,3], Aidin Razavi[2], Jan Carlsson[1,3,4] and Andrés Alayón Glazunov[1,5]
[1]Department of Electrical Engineering, Chalmers University of Technology,
Gothenburg, Sweden, madeleine.kildal@chalmers.se
[2]Ericsson Research, Ericsson AB, Gothenburg, Sweden
[3]RanLOS AB, Gothenburg, Sweden
[4]Provinn AB, Gothenburg, Sweden
[5]Department of Electrical Engineering, University of Twente, Enschede, The Netherlands

***Abstract*—In this paper we analyze three different verification procedures of the test zone in the Random Line-of-Sight measurement setup. The goal is to find a way to reduce the number of samples needed to estimate the standard deviation and the mean value within a circular test zone. It was found that more than 50 samples are needed to get reliable performance with the verification procedure using two orthogonal lines. However all three investigated methods work well, but the two other methods need more than 100 samples. This means that the samples can be taken within the test zone along two orthogonal lines, in a spiral shape, as well as a combination of these two methods, depending on the user's preference.**

***Index Terms*—vehicular, antenna, anechoic chamber, quiet zone, Random Line-Of-Sight, RLOS.**

I. Introduction

We are moving towards a society where more and more devices, among these also cars, will get a wireless connection. This development creates a need for reliable and efficient testing of the wireless communication to these devices. The Random Line-of-Sight (Random-LOS) environment was presented in [1] and [2] as a promising test environment for evaluation of the over-the-air (OTA) performance of the wireless communication for cars. The Random-LOS environment corresponds to an open environment, such as highways and rural areas, where there is a dominating line-of-sight (LOS) component between the communicating antennas. This LOS component will vary over time, as well as the angle of arrival of the incoming wave, as a car moves and turns around. The random angle of arrival introduce the randomness in the Random-LOS environment.

Initial simulations and measurements of the Random-LOS OTA measurement solution are presented in [3]–[9]. This paper is a continuation of the work presented in [5], [8] and [9]. Other OTA testing methods are, the multi-probe anechoic chamber [10], [11], the reverberation chamber [12] and the radiated two stage method [13].

The Random-LOS measurement setup consists of a cylindrical reflector with a linear array feed, see Fig. 1. The linear array feed used in this paper consists of 32 dual polarized bowtie antenna elements [14]. The test zone, where the variations of the field are sought to be minimized, is located in front of the reflector. It is defined by a circular area in the horizontal plane.

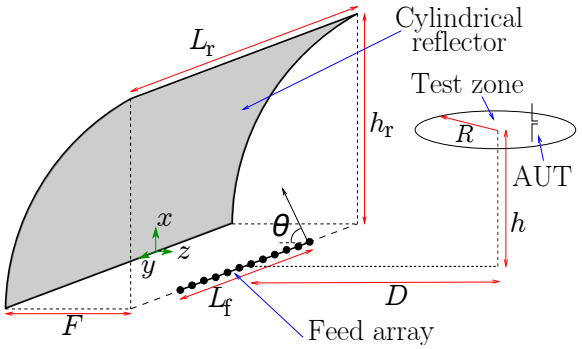

Fig. 1. Cylindrical reflector with linear feed array and the test zone for the AUT in front of the reflector.

In this paper, three different verification methods have been investigated. The goal of using a verification method is to verify that the test setup works as intended, with reasonably low uncertainty, in terms of standard deviation (STD) and mean value within the full test zone. The method should give a description of how the points should be sampled within the test zone, as well as providing the number of samples that are needed to get a good approximation of the STD and the mean value. As few samples as possible is desirable, to be able to reduce the measurement time.

II. Method

The cylindrical reflector has the length $L_r = 4\,\mathrm{m}$, height $h_r = 3\,\mathrm{m}$ and focal depth $f = 1.5\,\mathrm{m}$, see Fig. 1. The feed array consists of 32 dual polarized bowtie antennas centred in front of the reflector with an inter-element spacing of 10 cm. The feed array length is $L_f = 3.2\,\mathrm{m}$. The tilting of the bowtie antennas is defined by $\theta = 55\,^\circ$. The working frequency of the reflector with the linear bowtie feed is $1.5\,\mathrm{GHz} - 3\,\mathrm{GHz}$. The working frequency is somewhat larger than the frequency band for the bowtie array presented in [14], since the spacing between the elements has been reduced to 10 cm, compared to the previous 11 cm. The circular test zone of the Random-LOS measurement setup has a radius of R and is centred at

$y = 0\,\mathrm{m}$ and located in front of the cylindrical reflector in the yz-plane at the height h and the distance D.

A. Simulation

The simulations of the reflector and the field variations within the test zone have been performed using a Physical Optics (PO) algorithm implemented in Matlab. The code is described in detail in [8], but a summary is given next for the sake of completeness. From the embedded radiation pattern of the bowtie feed antennas, the incident magnetic field $\mathbf{H}^i$ on the reflector surface can be obtained. This field can be used to compute the PO current $\mathbf{J} = 2\hat{\mathbf{n}} \times \mathbf{H}^i$ in the center of each grid cell on the reflector surface. The PO current is then used to calculate the scattered field $\mathbf{E}^s$ from the reflector in the test zone using the formulas in [15, Sec. 4.2]. The total field $\mathbf{E}^t$ in the test zone is the sum of the scattered field $\mathbf{E}^s$ and the incident field to the test zone $\mathbf{E}^i$. The grid of the reflector is made up of squares with a side length of $\lambda/2$.

B. Verification method

A verification method is sought to verify the performance of the reflector within the test zone. The goal is to decrease the number of sample points in a real measurement scenario, which in turn would lead to a reduction in measurement time. The three considered verification methods describe three different ways of collecting the samples within the test zone, as well as how many samples that are needed. These methods are compared to each other and to a reference case. The reference case is the case when the full variation within the test zone is known, which is realized in the simulations with a uniform grid of sample points. The three verification methods that have been compared are two orthogonal lines, a spiral and a combination of these two. The number of sample points, N, needed within the three verification cases has been investigated as well. The comparison is made in terms of STD and mean value of the sample points.

For all the comparisons, the test zone has been located at $h = 1.6\,\mathrm{m}$, which is a typical height for the roof of the car, where the antenna is normally located. The distance from the feed array to the center of the test zone is $D = 4.5\,\mathrm{m}$. This distance was chosen according to the results in [16]. The comparisons are made at two frequencies, corresponding to two of the LTE frequency bands, LTE band 1 (2.1 GHz) and LTE band 7 (2.6 GHz).

1) Reference grid: The reference case is calculated from data points taken from a uniform rectangular grid with a grid spacing of $5\,\mathrm{cm}$, see Fig. 2(a). The spacing was chosen as half the wavelength of the upper operating frequency limit, 3 GHz, of the feed array. No significant change in STD and mean value was found when decreasing the grid spacing to $2\,\mathrm{cm}$, so it is assumed that a spacing of $5\,\mathrm{cm}$ is enough. A grid spacing of $5\,\mathrm{cm}$ within a test zone with radius $1\,\mathrm{m}$ corresponds to $N = 1257$ data points.

2) Two orthogonal lines: The first method is to sample the measurement points along two orthogonal lines in the test zone. The lines are aligned such that they go along the z-axis and parallel to the y-axis in Fig. 1. See a close up of the test zone in Fig. 2(b). There are $N/2$ sample points along each of the two lines. Only unique sample points are used, so if there are sample points occurring at the same location, then only one of them is used.

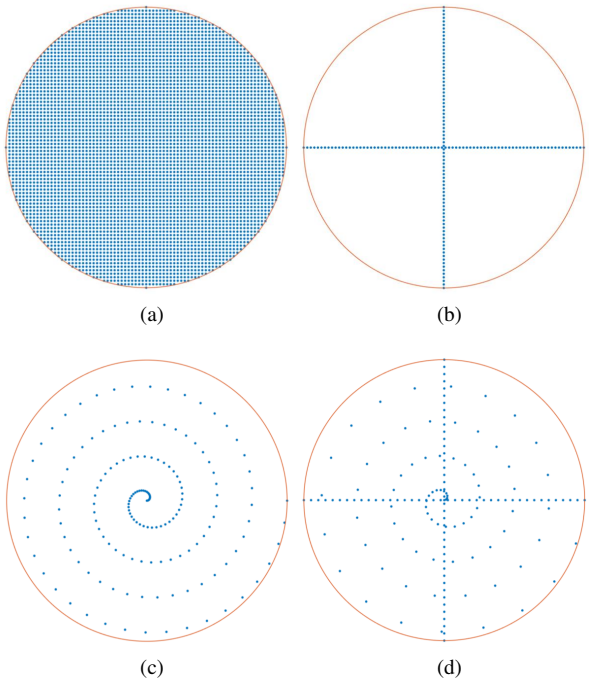

Fig. 2. Different ways of sampling the data points within the test zone, (a) uniform rectangular grid, (b) two orthogonal lines, (c) spiral, (d) two orthogonal lines and the spiral.

3) Spiral: The second method is to sample the measurement points along a spiral within the test zone. The number of full 2π-rotations within the test zone was set to 4. The N samples are then spaced evenly in both radius and azimuth angle, see Fig. 2(c).

4) Lines and spiral: The third method is to combine the two orthogonal lines and the spiral. Here, the number of sample points is divided with $N/4$ samples on each of the two orthogonal lines and $N/2$ samples on the spiral. The combination can be seen in Fig. 2(d). Only unique sample points are used, so if there are sample points occurring at the same location, then only one of them are used.

III. Results

The STD σ_{dB} has been calculated in dB according to the following formula [17]

$$\sigma_{\mathrm{dB}} = 5 \log \left(\frac{1+\sigma}{1-\sigma} \right) , \tag{1}$$

where σ is the STD of the normalized power in linear units, i.e.,

$$\sigma = \sqrt{\mathrm{VAR}\left\{ \frac{P}{\mathrm{MEAN}\{P\}} \right\}} , \tag{2}$$

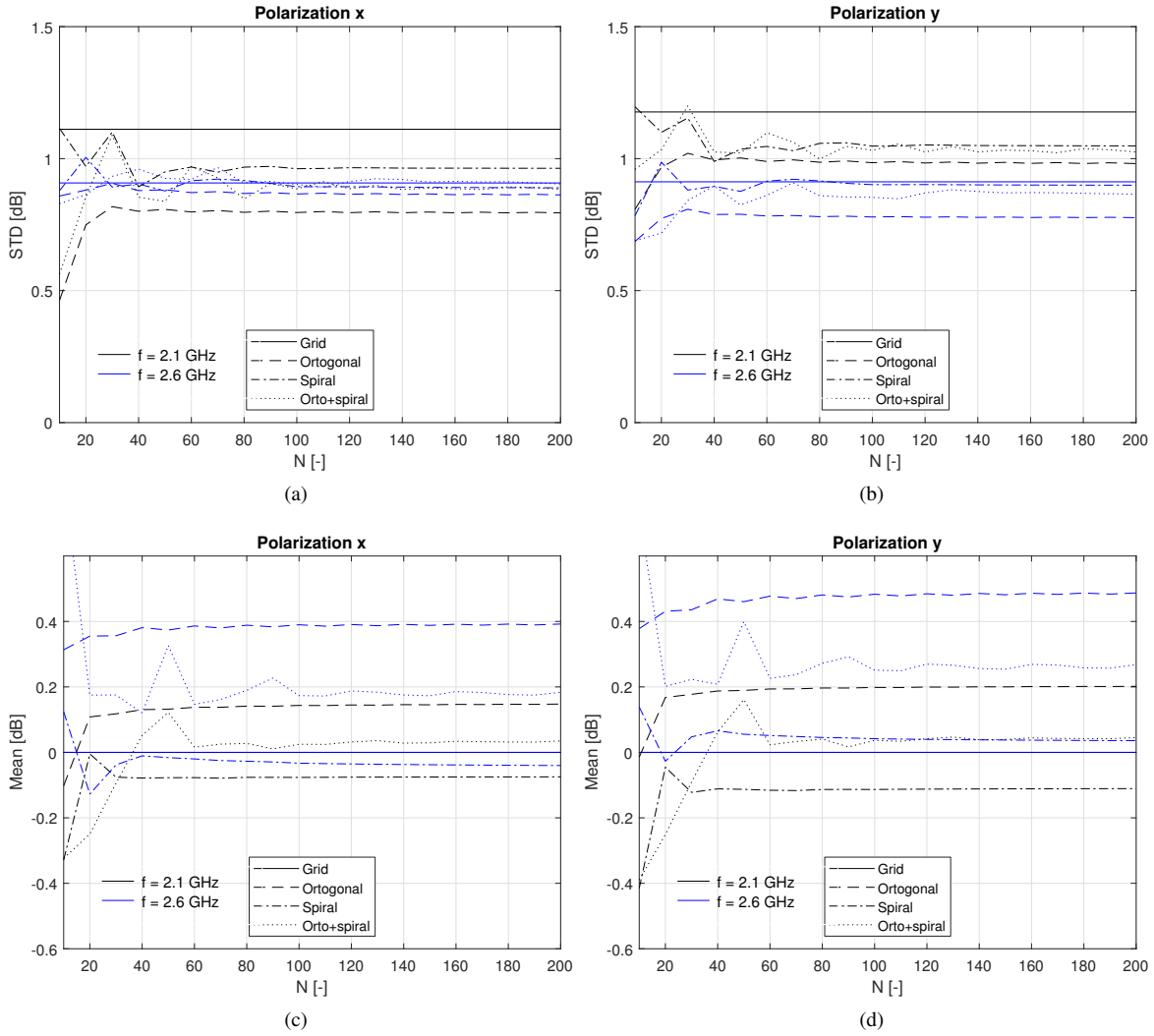

Fig. 3. Standard deviation and normalized mean value as a function the total number of sample points N. The solid lines correspond to the reference grid case, when using a uniform grid with $N = 1257$. The two solid lines in (c) and (d) are on top of each other. (a) Standard deviation for the x-polarization, (b) standard deviation for the y-polarization, (c) mean for the x-polarization and (d) mean for the y-polarization.

where $\mathrm{VAR}\{\cdot\}$ and $\mathrm{MEAN}\{\cdot\}$ are the sample variance and sample mean operations, respectively. P is the power and is defined as $P = |E_x|^2$ or $P = |E_y|^2$, where the subscript x corresponds to vertical polarization and subscript y corresponds to the horizontal polarization, see Fig. 1.

A. Number of sample points

The STD as a function of the number of sample points N for the three different verification methods can be seen in Fig. 3(a)-(b). The corresponding mean values are shown in Fig. 3(c)-(d). The mean value is shown as normalized mean, where the normalization factor is the mean value obtained using the reference grid for the two frequencies. This is the reason the two solid reference grid lines are on top of each other at zero mean. The reference grid has a spacing of $5\,\mathrm{cm}$ resulting in $N = 1257$ data samples. The test zone radius was $R = 1\,\mathrm{m}$. The difference between the two polarizations can be explained by the slightly different radiation pattern for the two polarizations of the feed array.

It can be seen that the two orthogonal lines converge fast to a stable value, and the lowest number of sample points to get reliable results is 50. The spiral case and the combined case both need more data points to converge. All three verification methods converge and do not change much in STD and mean value for a number of sample points larger than 100. Based on these results, it was decided to compare the verification methods using the same number of sample points $N = 128$.

B. Reference grid

The STD for the reference grid is shown as the solid lines in Fig. 4(a)-(b). The STD is plotted as a function of the test zone radius. The test zone radius has been increased in steps of $0.1\,\mathrm{m}$ from $0.1\,\mathrm{m}$ to $2\,\mathrm{m}$. The corresponding mean values are shown by the solid lines in Fig. 4(c)-(d). The mean values are normalized to the mean value obtained for the reference

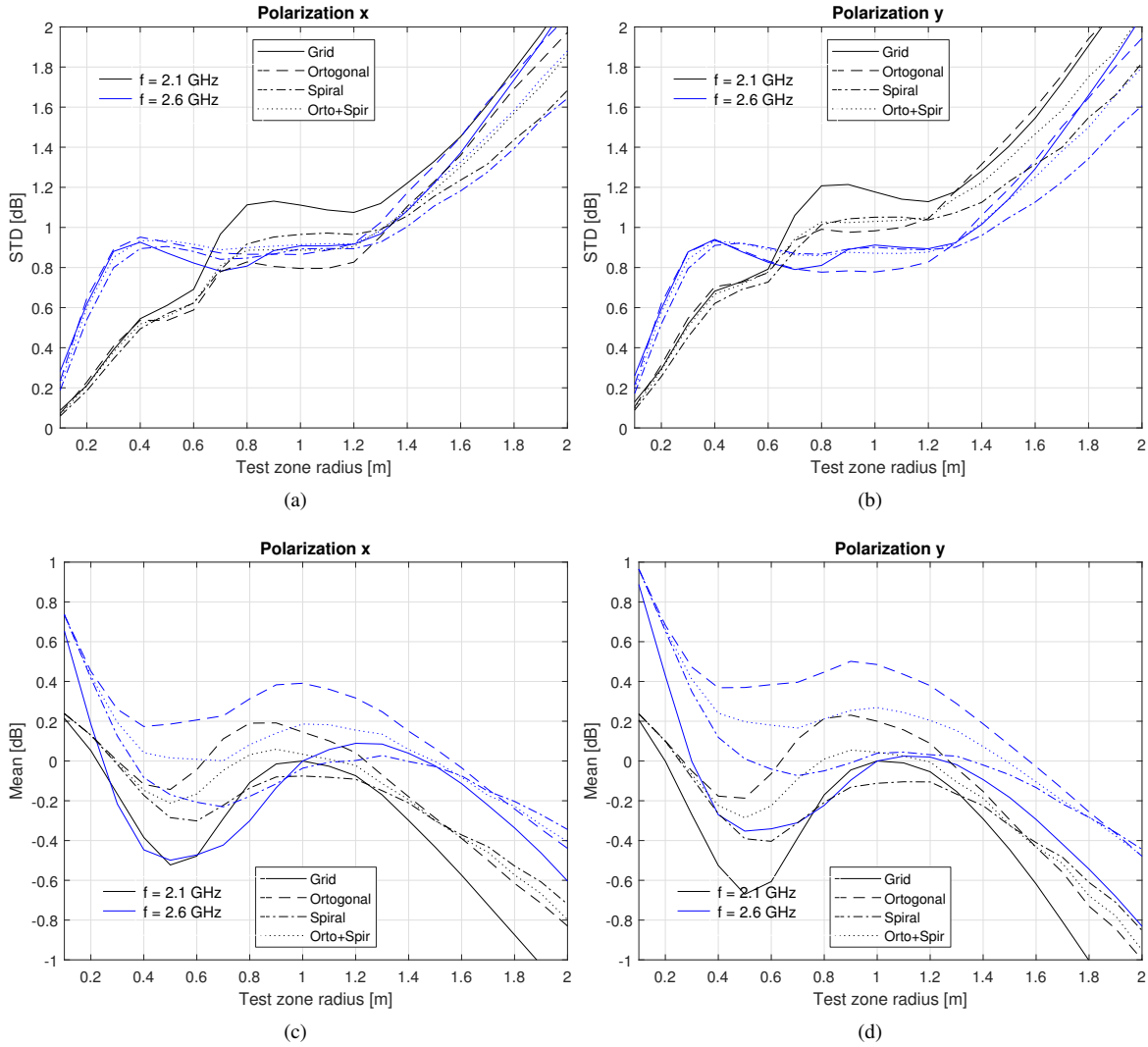

Fig. 4. Standard deviation and mean value as a function of test zone radius for the different verification methods. (a) Standard deviation for the x-polarization, (b) Standard deviation for the y-polarization, (c) Normalized mean for the x-polarization and (d) Normalized mean for the y-polarization.

grid at $R = 1\,\mathrm{m}$ for the corresponding frequency. Since the values are calculated based on a uniform grid, the number of sample points will increase as the test zone radius. The number of data points will be larger than 100 for a radius larger than $0.3\,\mathrm{m}$.

C. Verification methods

The comparison of the STD between the verification methods and the reference are presented in Fig. 4(a)-(b) as a function of test zone radius for two frequencies, $f = 2.1\,\mathrm{GHz}$ and $f = 2.6\,\mathrm{GHz}$. The corresponding comparison of mean value for the two different polarizations are presented in Fig. 4(c)-(d). The mean values are normalized to the mean value obtained for the reference grid at $R = 1\,\mathrm{m}$ for each polarization and frequency. The STD and mean values for all radii have been calculated using the same number of sample points, $N = 128$. Thus the grid spacing will be different for the different radii.

It can be seen that the STD for all verification methods show good agreement with the reference grid when $R < 1.2\,\mathrm{m}$. It can also be seen that the spiral case starts showing a different trend, with lower STD than the reference for test zone radii larger than $1.2\,\mathrm{m}$. The two orthogonal lines and the combined case show a more correct trend for the larger test zone radii.

All verification methods behaves similar to the reference grid, but with some slight shift in absolute value. For the mean value the spiral case has better agreement than the others for $R < 1.5\,\mathrm{m}$, whereas the other two methods have better agreement for larger test zone radii.

Looking at both STD and mean values for the whole test zone radius range ($0.1\,\mathrm{m} < R < 2\,\mathrm{m}$) the combined spiral and lines verification method works the best, with the closest performance to the reference grids. However, all three methods work well as verification methods.

IV. Conclusion

It has been found that all three methods that have been investigated work as verification methods for the Random-LOS measurement setup. The verification method with the two orthogonal lines works the best when considering both the overall performance and the lowest number of sample points needed for accurate performance. The number of sample points needed to trust the verification method in this case was 50. A slightly better performance can be achieved with the combined method, spiral and two orthogonal lines, if the measurement time is not crucial. In this case would the number of sample points need to be more than 100.

Since all three methods work well it can be decided by the user which one is the most practical to use at a given time. This means that we can use these verification methods to find the STD and mean within the test zone, without measuring the full test zone field variation.

Acknowledgment

The project is partly supported by the Swedish Research Council VR, through an industrial PhD project.

References

[1] P.-S. Kildal and J. Carlsson, "New approach to OTA testing: RIMP and pure-LOS reference environments and a hypothesis," in *2013 7th European Conference on Antennas and Propagation (EuCAP)*, Apr. 2013, pp. 315–318.

[2] P.-S. Kildal, A. A. Glazunov, J. Carlsson, and A. Majidzadeh, "Cost-effective measurement setups for testing wireless communication to vehicles in reverberation chambers and anechoic chambers," in *2014 Conference on Antenna Measurements Applications (CAMA)*, Nov. 2014, pp. 1–4.

[3] P.-S. Kildal, "Methods and apparatuses for testing wireless communications to vehicles," Jan. 2014, patent application number PCT/EP2014/054620. Applicant is Kildal Antenn AB.

[4] M. S. Kildal, J. Kvarnstrand, J. Carlsson, A. A. Glazunov, A. Majidzadeh, and P.-S. Kildal, "Initial measured OTA throughput of 4g LTE communication to cars with roof-mounted antennas in 2d random-LOS," in *2015 International Symposium on Antennas and Propagation (ISAP)*, Nov. 2015, pp. 1–4.

[5] A. A. Glazunov, A. Razavi, and P.-S. Kildal, "Simulations of a planar array arrangement for automotive Random-LOS OTA testing," in *2016 10th European Conference on Antennas and Propagation (EuCAP)*, Apr. 2016, pp. 1–5.

[6] A. Razavi, A. A. Glazunov, P.-S. Kildal, and R. Maaskant, "Array-fed cylindrical reflector antenna for automotive OTA tests in Random Line-Of-Sight," in *2016 10th European Conference on Antennas and Propagation (EuCAP)*, Apr. 2016, pp. 1–4.

[7] M. S. Kildal, A. A. Glazunov, J. Carlsson, and A. Majidzadeh, "Evaluation of a simplified Random-LOS measurement setup for characterizing antennas on cars," in *2017 11th European Conference on Antennas and Propagation (EUCAP)*, Mar. 2017, pp. 3007–3011.

[8] A. Razavi, A. A. Glazunov, S. M. Moghaddam, R. Maaskant, and J. Yang, "Characterization Method of an Automotive Random-LOS OTA Measurement Setup," *Progress In Electromagnetics Research C*, vol. 2018, no. 84, pp. 47–60, 2018.

[9] M. S. Kildal, J. Carlsson, and A. A. Glazunov, "Measurements and Simulations for Validation of the Random-LOS Measurement Accuracy for Vehicular OTA Applications," *IEEE Transactions on Antennas and Propagation (Early Access)*, pp. 1–1, Sep. 2018.

[10] W. Fan, F. Sun, J. Ø. Nielsen, X. Carreño, J. S. Ashta, M. B. Knudsen, and G. F. Pedersen, "Probe Selection in Multiprobe OTA Setups," *IEEE Transactions on Antennas and Propagation*, vol. 62, no. 4, pp. 2109–2120, Apr. 2014.

[11] W. Fan, P. Kyösti, J. O. Nielsen, and G. F. Pedersen, "Wideband MIMO Channel Capacity Analysis in Multiprobe Anechoic Chamber Setups," *IEEE Transactions on Vehicular Technology*, vol. 65, no. 5, pp. 2861–2871, May 2016.

[12] P.-S. Kildal, C. Orlenius, and J. Carlsson, "OTA Testing in Multipath of Antennas and Wireless Devices With MIMO and OFDM," *Proceedings of the IEEE*, vol. 100, no. 7, pp. 2145–2157, Jul. 2012.

[13] W. Yu, Y. Qi, K. Liu, Y. Xu, and J. Fan, "Radiated Two-Stage Method for LTE MIMO User Equipment Performance Evaluation," *IEEE Transactions on Electromagnetic Compatibility*, vol. 56, no. 6, pp. 1691–1696, Dec. 2014.

[14] S. M. Moghaddam, A. A. Glazunov, and J. Yang, "Wideband Dual-Polarized Linear Array Antenna for Random-LOS OTA Measurement," *IEEE Transactions on Antennas and Propagation*, vol. 66, no. 5, pp. 2365–2373, May 2018.

[15] P.-S. Kildal, *Foundations of Antenna Engineering - A Unified Approach for Line-Of-Sight and Multipath*, 2015th ed. Gothenburg, Sweden: Kildal Antenn AB, Mar. 2017, available at www.kildal.se.

[16] M. S. Kildal, A. A. Glazunov, and J. Carlsson, "A Numerical Analysis of the Random-LOS Measurement Accuracy for Vehicle Applications," in *2018 12th European Conference on Antennas and Propagation (EUCAP)*, London, U.K., Apr. 2018.

[17] P.-S. Kildal, X. Chen, C. Orlenius, M. Franzén, and C. Patané, "Characterization of Reverberation Chambers for OTA Measurements of Wireless Devices: Physical Formulations of Channel Matrix and New Uncertainty Formula," *IEEE Transactions on Antennas and Propagation*, vol. 60, no. 8, pp. 3875–3891, Aug. 2012.